

Morphological, Thermal, and Mechanical Characterization of Bio-Based High-Density Polyethylene / Biopolyamide 6.10 Blends Compatibilized with PE and SEBS Functionalized With Maleic Anhydride

Jamile Almeida Vieira^{a*} , Zora Ionara Gama dos Santos^a, Marcelo Massayoshi Ueki^a 

^aUniversidade Federal de Sergipe, Departamento de Ciência e Engenharia dos Materiais, Avenida Marechal Rondon, Jardim Rosa Elze, São Cristóvão, SE, Brasil.

Received: June 16, 2023; Revised: October 12, 2023; Accepted: October 20, 2023

This work reports the study of the compatibilization of the blend of biopolyethylene and biopolyamide 6.10, both biobased. In this work, two polymers functionalized with maleic anhydride (PE-g-MA and SEBS-g-MA) were used as compatibilizers of the blend. The blends were prepared in a single screw extruder and subsequently molded by injection. SEM results showed the immiscibility of the Bio-HDPE/PA6.10 blend. With the addition of the compatibilizers, a compatible interface was formed. The DSC results showed changes in the crystallization behavior of the two phases with the addition of compatibilizers. FTIR results suggested that there was a reaction between the maleic anhydride of the compatibilizers and the terminal amino groups of the polyamide. The blend containing PE-g-MA showed greater stiffness, with an increase in the modulus of elasticity in relation to Bio-HDPE, while the blends containing SEBS-g-MA showed excellent resistance to impact and high elongation at break.

Keywords: *Biopolymers, reactive compatibilization, bio-based high-density polyethylene, biopolyamide 6.10, SEBS-g-MA, PE-g-MA.*

1. Introduction

In recent decades, there has been an increase in legislative actions about environmental protection, sustainability, and waste management. In 2015, the United Nations established the 2030 Agenda for Sustainable Development, called “Transforming our world”. The agenda established 17 Sustainable Development Goals (SDGs) which include topics such as climate, energy, oceans, science, and technology. According to reports on the latest research and sustainability initiatives within each area of the SDGs, materials science contributes to achieving some goals, such as sustainable cities and communities (SDG 11), responsible consumption and production (SDG 12) and climate action (SDG 13)^{1,2}.

In this context, there is currently a strong incentive to produce polymers with a lower impact on the environment, and among the candidate technologies are bio-based polymers, which are polymers totally or partially derived from renewable raw materials. Renewable resources, especially biomass sources such as sugar cane and vegetable oils, have emerged as potential sustainable alternatives to produce monomers. Bio-based polymers are fully recyclable and contribute to reducing the carbon footprint, as the manufacturing process involves fewer greenhouse gas emissions, and in some cases, it is possible to capture CO₂ from the atmosphere. One example is green polyethylene (PE), which uses ethanol from sugar cane as a raw material for its production. For every kilo of green PE produced, around 2 kg of CO₂ is captured from the atmosphere²⁻⁴.

In terms of mechanical properties, which are the main performance metrics for materials, bio-based polymers have similar or even superior properties compared to petrochemical polymers, considering each application. Green PE has the same properties as fossil-based polyethylene, while polyamide (PA) 6.10 replaces PA 12 in the manufacturing of parts for the automotive sector. PA 6.10 is a polymer composed of 64% renewable raw materials derived from castor oil⁵⁻⁸.

Blends of PE and PA produced from fossil raw materials are mixtures of great industrial importance and have been used commercially in the preparation of filaments, plastic containers, and molding resins. In view of the application potential of these blends, it is possible to replace PE from fossil sources with green PE, since their properties are similar, as well as the possibility of replacing petrochemical PA with other PAs from renewable sources^{9,10}.

In addition, the presence of PA in a PE matrix can improve its tensile mechanical properties, such as yield strength and modulus of elasticity, as well as providing greater thermal and dimensional stability. However, since they are immiscible polymers, their blends reprocessed by melting show phase separation and poor mechanical properties. The mechanical properties of immiscible blends can be improved using compatibilization methods. Compatibilization is a process of modifying the interfacial properties of the blend, which leads to the stabilization of morphology, promoted by the reduction of interfacial tension⁹⁻¹⁸.

In view of the above, the aim of this work was to improve the mechanical properties of the green high-density polyethylene (Bio-HDPE) blend with polyamide 6.10 partially from a renewable source (PA 6.10).

*e-mail: jamisantos.ja@gmail.com

To minimize the effects of immiscibility, the Bio-HDPE/PA6.10 blend was prepared using styrene-poly(ethylene-*co*-butylene)-styrene blocks functionalized with maleic anhydride (SEBS-*g*-MA) and high-density polyethylene functionalized with maleic anhydride (PE-*g*-MA) as compatibilizing agents. The morphological, thermal, and mechanical properties of the non-compatibilized and compatibilized blends were evaluated via Scanning Electron Microscopy (SEM), Differential Scanning Calorimetry (DSC) and mechanical tensile and impact tests, respectively. Fourier Transform Infrared Spectroscopy (FTIR) analysis was carried out to characterize the chemical structure of the blends.

2. Materials and Methods

2.1. Materials

For the formulation of the blends, polyamide 6.10 (PA6.10) was used, donated by EVONIK Industries AG, trade name VESTAMID Terra HS18, with a density of 1.07 g/cm³. The green polyethylene (Bio-HDPE) was supplied by Braskem under the tradename SHC7260, with a flow index of 7.2 g/10min and density of 0.959 g/cm³. The polymers used as compatibilizing agents for the blend were high-density polyethylene grafted with maleic anhydride (PE-*g*-MA), trade name OREVAC 18507, donated by Arkema, with a flow index of 5 g/10min (190 °C/2.16 kg) and styrene-block-poly(ethylene-*co*-butylene)-block-styrene grafted with maleic anhydride (SEBS-*g*-MA), trade name Kraton FG1901, donated by Kraton, with a flow index of 14 - 28 g/10 min (230 °C/5.0 kg). The maleic anhydride content is 1.4 - 2.0%.

2.2. Blends Preparation

Due to the hygroscopic characteristic of polyamide, the biopolyamide 6.10 pellets were dried in a circulating air oven at a temperature of 100 °C for a period of 4 hours. After this period, the pellets were placed in a vacuum oven to continue the drying process at a temperature of 120 °C for 4 hours. After drying, the production of the blends was carried out by the extrusion process, in a single screw extruder, screw diameter of 30 mm and L/D = 34, Wortex brand, model WEX30, operating with screw rotation speed of 70 rpm. The composition of the blends is indicated in Table 1. The temperature in each zone was: Z1 (feed): 175 °C; Z2: 210 °C; Z3: 225 °C; Z4: 230 °C; and Z5 (head): 220 °C.

The blends obtained by the extrusion process were dried in a circulating air oven at 100 °C for 4 hours.

Subsequently, they were injection molded and specimens were obtained in the form of a tie, in accordance with ISO 527 for carrying out the tensile tests. The injection molding machine used was a BATTENFELD brand and model HM 45/210 and has molds with Z-shaped distribution channels with a blade-shaped injection point, meeting the ISO 527 - (1993) configuration (mold/dimensioning). The temperature profile was: Z0.1 (nozzle): 230 °C; Z1: 230 °C; Z2: 200 °C; Z3 (feed): 175 °C, with holding pressure 700 bar, injection pressure 800 bar and cooling cycles lasting 15 seconds. In this research work, blends with SEBS-*g*-MA will be called SBMA, and blends with PE-*g*-MA will be called PEMA. Bio-HDPE/PA6.10 is the non compatibilized blend.

2.3. Blends Characterizations

2.3.1. Mechanical characterization

For the uniaxial tensile test of the specimens, a universal mechanical testing machine from the INSTRON, model 3367, was used. This test was carried out in accordance with the ISO 527-1 1993 standard. The test speed was 50mm/min, the distance between the grips was 115 mm and the specimen dimensions were 4.0 mm thick and 10.2 mm wide. The data extracted from the tensile test were modulus of elasticity, yield stress and deformation at break of blends and pure polymers. The notched IZOD impact test was carried out using the IZOD impact testing machine for polymers, INSTRON, model CEAST 9050. The test hammer energy was 2.7 J. The impact strength calculations were performed according to the ISO 180 standard.

2.3.2. Morphological characterization

The morphology of the blends was observed using a Carry Scope Scanning Electron Microscope (SEM), model JCM-5700. The samples were notched using the Izod impact test hammer and vacuum coated with gold. The images were obtained from the secondary electron detector. Electron acceleration voltages of 10 kV and 20 kV and 5000 x magnification were used. Image J software was used to analyze the droplet size of the dispersed phase.

2.3.3. Thermal characterization

The thermal analyzes were carried out using the Differential Scanning Calorimeter (DSC) NETZSCH DSC 200 F3 Maia, to identify the melting temperatures (T_m), crystallization temperatures (T_c), enthalpy of crystallization (ΔH_c), and enthalpy of fusion (ΔH_m) related to the pure polymers and the blends.

Table 1. Blends composition.

Samples	Composition			
	Bio-HDPE (wt%)	PA6.10 (wt%)	PE- <i>g</i> -MA (wt%)	SEBS- <i>g</i> -MA (wt%)
Bio-HDPE/PA6.10	70	30	-	-
3% PEMA	70	30	3	-
6% PEMA	70	30	6	-
3% SBMA	70	30	-	3
6% SBMA	70	30	-	6
3% PEMA + 3% SBMA	70	30	3	3

Samples weightings from 5 - 6 mg sealed in aluminum pans were used. During the test, the samples were subjected to a cooling cycle and two heating cycles, with a heating and cooling rate of 10 °C/min and a temperature ranging from 40 to 240 °C. The analysis was carried out with a nitrogen atmosphere. The degree of crystallinity ($w_{c,h}$) of Bio-HDPE and PA6.10 components was determined using the Equation 1:

$$w_{c,h} = \frac{\Delta H_m}{\varphi(1-w_f) \times \Delta H_m^0} \times 100 \% \quad (1)$$

where ΔH_m is the measured enthalpy of fusion from the second heating cycle, ΔH_m^0 is the enthalpy of fusion assuming 100% crystallinity, being 293 J/g for HDPE⁷ and 254 J/g for PA6.10⁸, φ is the weight fraction in the blends or composites, and w_f is the weight fraction of block copolymer.

2.3.4. Structural characterization

Fourier transform infrared spectra of the blends were recorded using a Thermo Scientific spectrometer, model Nicolet™ iS20, with the Attenuated Total Reflection (ATR) technique.

The spectra were obtained by superposition of 32 scans with a resolution of 2 cm⁻¹ and an operating range of 3950 to 455 cm⁻¹.

3. Results and Discussion

3.1. SEM analysis

Representative micrographs of the fracture surface of the 70Bio-HDPE/30PA6.10 blend and of the compatible blends are presented in Figure 1, obtained by means of Scanning Electron Microscopy (SEM). Figure 1a referring to the non-compatible blend shows a two phase morphology, consisting of the polyamide phase dispersed in fibrous form in the Bio-HDPE matrix phase. The dispersed phase has a smooth surface, which indicates that there was no adhesion between the two phases, due to their immiscibility. It can be observed that the addition of small amounts of PE-g-MA and SEBS-g-MA (Figures b-f) promoted adhesion of the phases, and roughness can be observed on the surface of the dispersed phase.

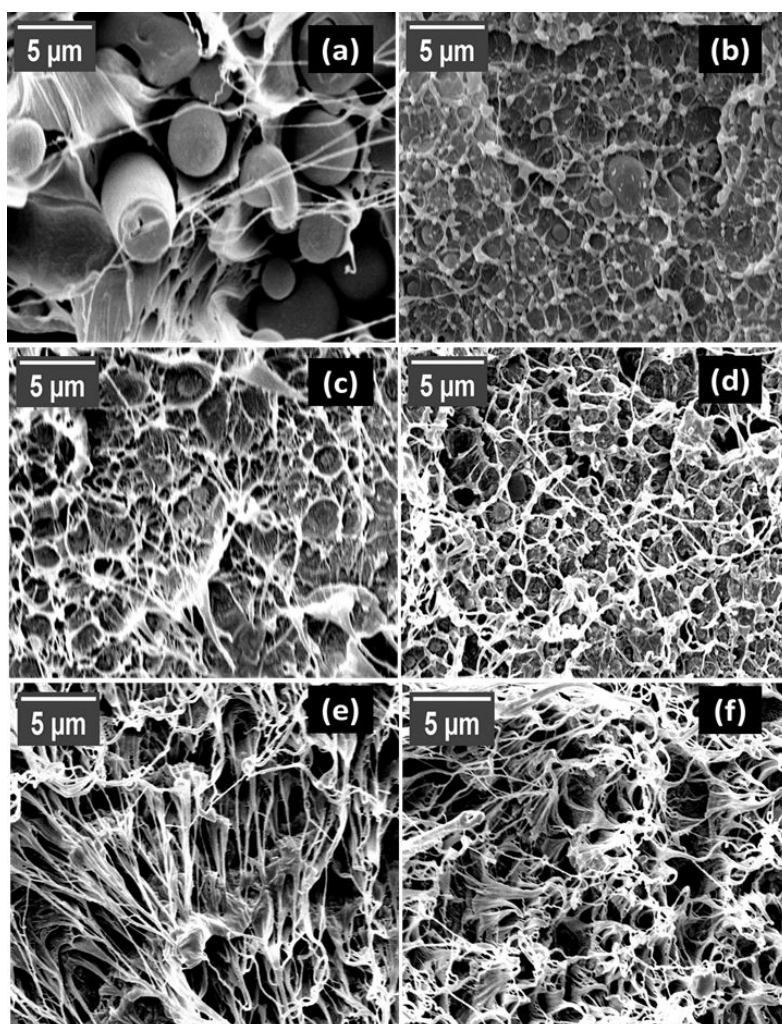


Figure 1. SEM micrographs of fractured surface of PE/PA (a) without and (b) with compatibilizer 3% PE-g-MA (c)6% PE-g-MA (d) 3% SEBS-g-MA; (e) 6% SEBS-g-MA and (f) 3% PE-g-MA + 3% SEBS-g-MA magnification 5000×.

There was also a notable droplet size reduction from the PA6.10 phase. The average droplet size of the dispersed phase in the incompatible blend is approximately 3.7 μm . In the blend with 3% PE-g-MA, the average size of the PA6.10 droplets became 1.2- μm , and in the blend with 3% SEBS-g-MA, the average size became 1.0 μm . These results indicate the occurrence of chemical reactions between the carboxylic groups present in PE-g-MA and SEBS-g-MA and the terminal amino groups of the polyamide. This reaction forms a copolymer *in situ* during blend processing (PE-g-PA or SEBS-g-PA). Figure 2 shows the proposed mechanism for the reaction. The copolymer formed acts as a compatibilizer at the blend interface, reducing the interfacial tension and promoting adhesion between the matrix phase and the dispersed phase. The result is a reduction in the size of the dispersed phase droplets and stabilization of the morphology, preventing coalescence.

3.2. DSC analysis

The influence of compatibilization agents addition on the thermal characteristics of the blend components was assessed by DSC measurements. Table 2 summarizes the melting temperature (T_m) values obtained in the second heating scans, the crystallization temperature (T_c) values obtained during the cooling scan, and the degree of crystallinity ($w_{c,h}$).

The DSC thermograms shown in Figure 3 and Figure 4 refer to the cooling and second heating of Bio-HDPE, PA6.10 and their blends respectively. The cooling curves referring to Bio-HDPE (Figure 3a) show that the presence of PA6.10 causes a displacement of the Bio-HDPE crystallization onset temperature to higher values. PA6.10 can act as a precursor core for crystal formation, decreasing the energy needed to initiate the crystallization process.

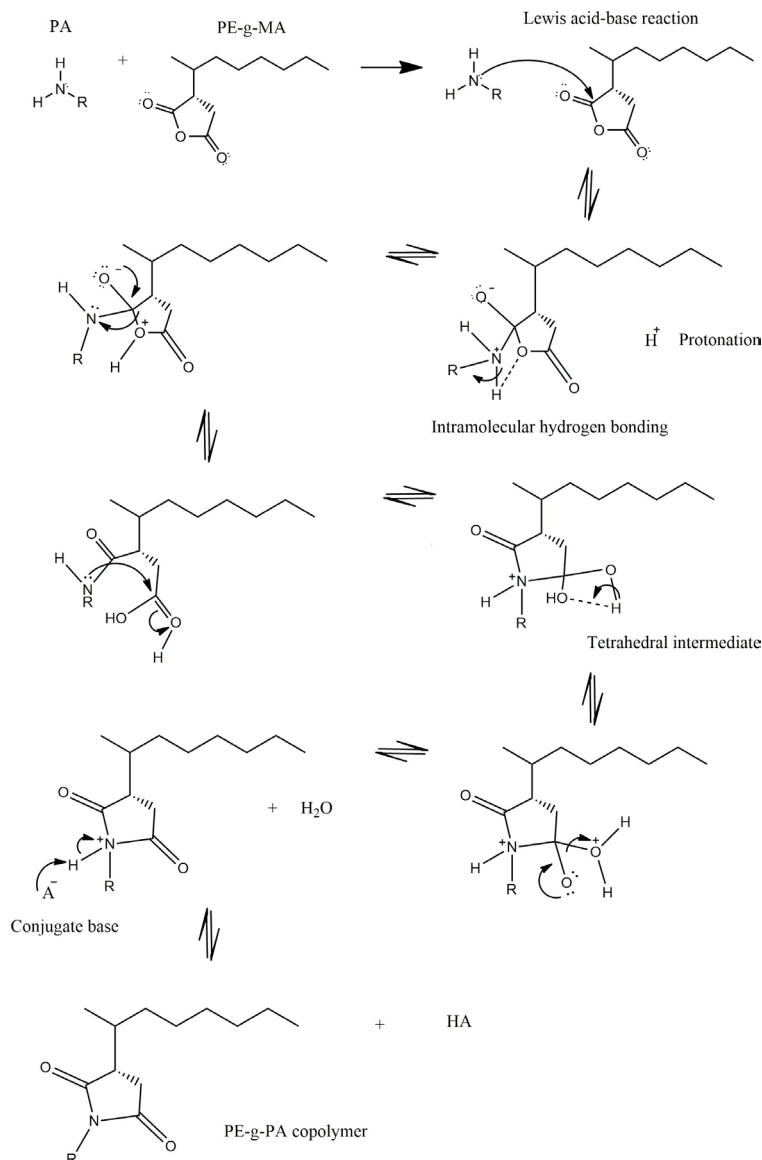


Figure 2. Proposed reaction mechanism for *in situ* copolymer formation.

The blends with 3% and 6% of PE-g-MA showed a similar behavior, following the trend of advancing the temperature at the beginning of the crystallization of Bio-HDPE. Observing the cooling curves referring to blends with SEBS-g-MA, shown in Figure 3a, the crystallization of Bio-HDPE is delayed in the presence of this copolymer.

The data shown in Table 2 show that the degree of crystallinity of Bio-HDPE increased in the Bio-HDPE/PA6.10 blend. The addition of PE-g-MA and SEBS-g-MA to the blend results in a reduction in the degree of crystallinity of Bio-HDPE, this effect being

more pronounced in Bio-HDPE/PA6.10/6% SEBS-g-MA and Bio-HDPE/PA6.10/3% PE-g-MA/3% SEBS-g-MA systems. The reduction in the degree of crystallinity of Bio-HDPE indicates interaction between the phases of the blend.

The cooling curves of the blends, referring to PA6.10, are shown in Figure 3b. It is observed that there is a displacement of the crystallization peak towards higher temperatures in the blend Bio-HDPE/PA6.10. In the other systems, the trend observed in the curves is a delay in the beginning of the PA6.10 crystallization process.

Table 2. Values of T_m^{1*} , T_m^{2*} , T_c^1 , T_c^2 , and of the samples.

Samples	T_m^1 (°C)	T_m^2 (°C)	T_c^1 (°C)	T_c^2 (°C)	(%)	(%)
Bio-HDPE	135.4±0.8	-	114.2±1.1	-	64.9±0.0	-
PA6.10	-	226.2±0.3	-	192.5±0.2	-	34.5±1.3
Bio-HDPE/PA6.10	136.5	224.2	112.9	195.3	68.1	18.1
3% SBMA	136.5±0.2	224.6±0.3	112.8±0.7	193.6±0.2	62.8±3.3	16.9±0.6
3% PEMA	135.1±0.1	224.2±0.0	114.9±0.2	195.3±0.2	63.0±0.4	18.7±0.1
6% PEMA	135.8±0.2	224.5±0.1	113.9±0.4	194.1±0.0	63.8±1.1	18.8±0.1
6% SBMA	137.9±1.3	225.0±0.5	111.7±1.0	192.0±0.6	54.9±1.9	13.8±0.2
3% PEMA + 3% SBMA	137.6±0.3	224.7±0.2	112.6±0.2	192.8±0.2	50.5±1.4	13.8±0.7

¹ The index for the Bio-HDPE phase. ² The index for the PA6.10 phase.

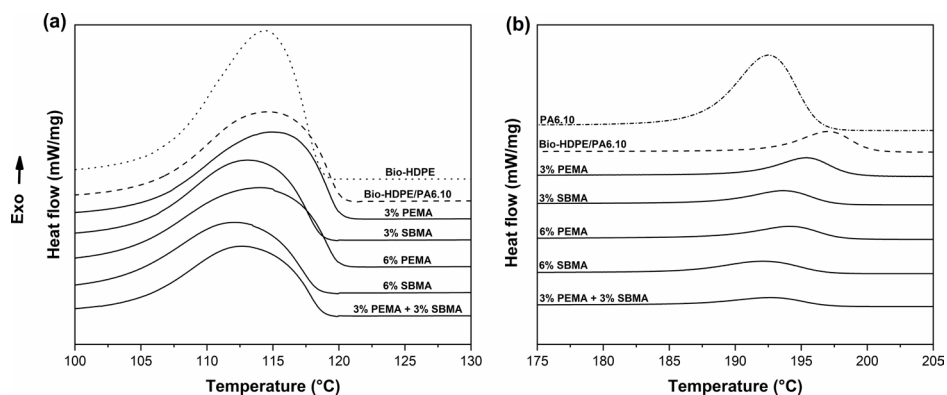


Figure 3. DSC cooling thermograms of the Bio-HDPE, PA6.10, and blends; (a) Bio-HDPE phase (b) PA6.10 phase.

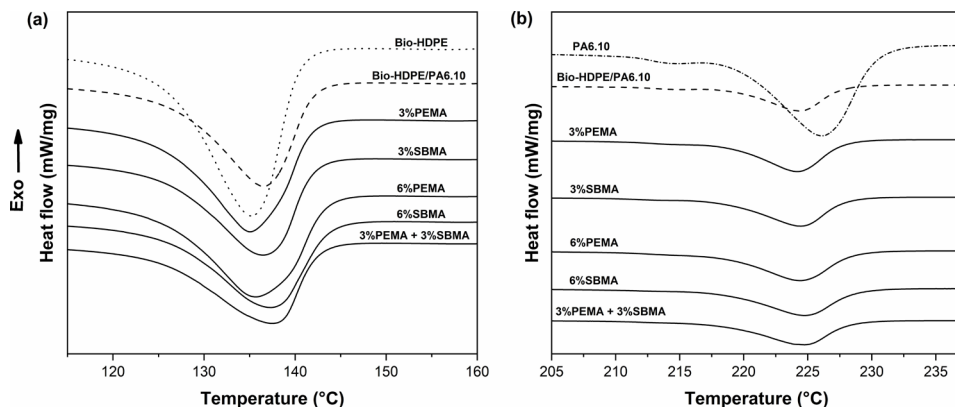


Figure 4. DSC thermograms of the Bio-HDPE, PA6.10, and blends; (a) endothermic process Bio-HDPE phase (b) endothermic process PA6.10 phase.

The degree of crystallinity of PA6.10 in these systems also showed a pronounced reduction in relation to the degree of crystallinity of PA6.10 in the Bio-HDPE/PA6.10 blend. These results indicate that in these systems, chemical reactions may have occurred between the maleic anhydride groups and the amine groups, forming the copolymer *in situ*. This could modify the crystallization process of PA6.10.

The occurrence of chemical reactions impairs crystallization by reducing chain mobility. In this case, a greater supercooling is necessary for nucleation to begin to occur. As a result, there is a displacement of the peak referring to the exothermic process to lower temperature values. This displacement can lead to a decrease in crystallinity, as the amorphous chain has less mobility to join the crystalline phase^{19,20}.

In the Bio-HDPE/PA6.10/6%SEBS-*g*-MA and Bio-HDPE/PA6.10/3%PE-*g*-MA + 3%SEBS-*g*-MA blends, a widening and slight reduction in peak height is observed, accompanied by a slight shift to lower temperatures. These results show an increase in interactions between the Bio-HDPE and PA6.10 phases. Similar results were observed by Liu et al.²¹ in an HDPE/PA6/SEBS-*g*-MA (80/20/6) system.

Heating thermograms in Figure 4 show a slight increase between 1 °C – 2 °C in the T_m of Bio-HDPE in blends containing SEBS-*g*-MA, when compared to the T_m of pure

Bio-HDPE. Possibly there was a favoring for the formation of a more organized crystalline structure of Bio-HDPE in these blends, increasing the melting temperature.

3.3. FTIR analysis

The FTIR spectra of Bio-HDPE, PA 6.10 and the Bio-HDPE/PA 6.10 blend are shown in Figure 5a. The spectrum of Bio-HDPE/PA 6.10 shows the characteristic absorption bands of Bio-HDPE and PA 6.10. The Bio-HDPE spectrum shows absorption bands at 2846 and 2914 cm⁻¹ corresponding to the CH₂ stretching vibration. The absorption bands at 1462 and 1472 cm⁻¹ are attributed to the CH₂ bending vibration. The absorption bands at 719 and 730 cm⁻¹ correspond to the CH₂ rocking vibration. The PA 6.10 spectrum shows absorption bands at 3297, 2921, 2850 and 1632 cm⁻¹, corresponding to N-H stretching vibration, antisymmetric CH₂ stretching, symmetric CH₂ stretching and C=O stretch vibration of monosubstituted amide, respectively. The absorption bands at 1539, 1465 and 1238 cm⁻¹ are attributed to the trans amide C-N-H bend vibration (amide II band), cis amide C-N-H bend, and the amide III band referring to the C-N-H bend, respectively. The spectrum of PA 6.10 also shows antisymmetric C-N stretching vibration (1180 cm⁻¹), C-C stretching vibration (937 cm⁻¹), and C-N deformation vibration (582 cm⁻¹).

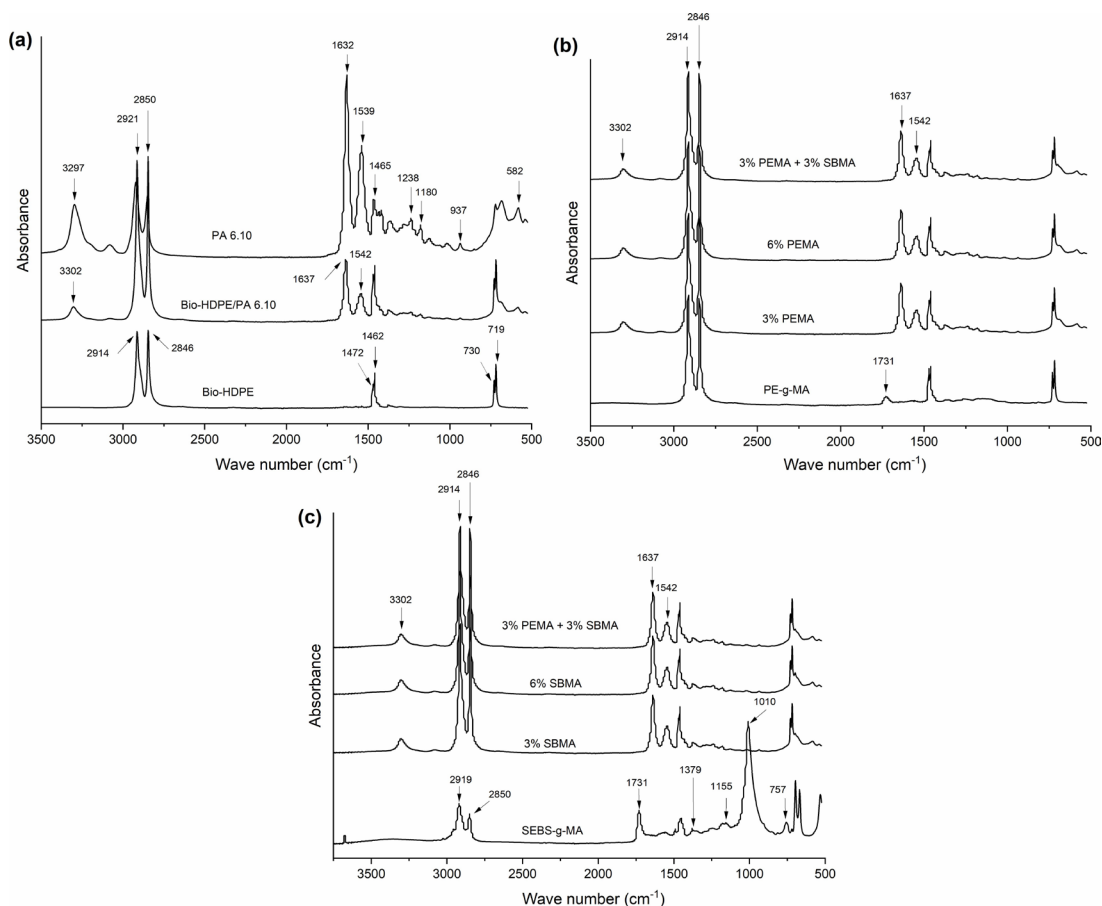


Figure 5. FTIR spectrum of: a) Bio-HDPE, PA 6.10, and Bio-HDPE/PA 6.10 blend; b) PE-*g*-MA, and the blends with 3% and 6% of the PE-*g*-MA; and c) SEBS-*g*-MA, and the blends with 3% and 6% of the SEBS-*g*-MA.

Figure 5b shows the absorption spectrum of PE-g-MA and Bio-HDPE/PA 6.10/PE-g-MA blends. It is observed that PE-g-MA presents absorption bands characteristic of Bio-HDPE at 2846, 2914, 1462, 1472, 719 and 730 cm^{-1} . The absorption band at 1731 cm^{-1} is related to the C=O vibration of the anhydride group. The blend spectra show characteristic absorption bands for Bio-HDPE and PA 6.10. However, the absorption band at 1731 cm^{-1} does not appear in the spectra of blends with PE-g-MA.

Figure 5c shows the characteristic absorption spectrum of SEBS-g-MA and Bio-HDPE/PA 6.10/SEBS-g-MA blends. The SEBS-g-MA spectrum shows symmetrical (2850 cm^{-1}) and antisymmetric (2921 cm^{-1}) CH_2 stretching vibration. The absorption band at 1379 cm^{-1} refers to the deformation of symmetric H-C-H and at 757 cm^{-1} refers to the rocking-twisting methylene vibration. The presence of the anhydride group is evidenced by the absorption bands at 1115, 1010 and 1731 cm^{-1} , the first two being attributed to the C-O-C stretch vibration of anhydrides and the last corresponding to the C=O vibration of anhydrides.

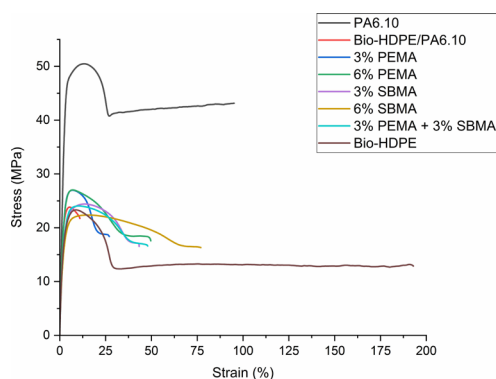


Figure 6. Curve of stress vs. strain of the blends.

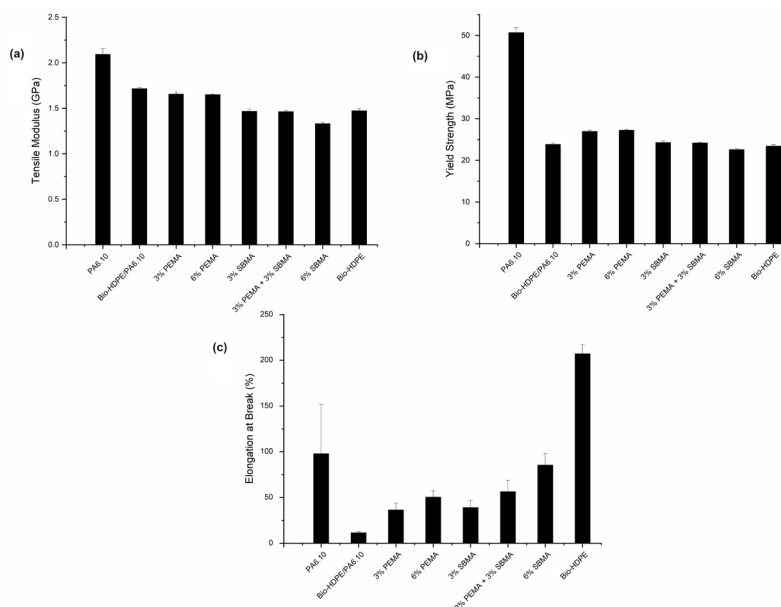


Figure 7. Mechanical properties of the blends; (a) tensile modulus, (b) yield strength, and (c) elongation at break.

It is observed in the absorption spectrum of the blends containing SEBS-g-MA the decrease in the intensity of the absorption band referring to the C-O-C stretch vibration of anhydrides (1010 cm^{-1}), as well as the reduction in the absorption band referring to the C=O vibration of anhydrides. The reduction in the intensity of the bands referring to the anhydride group (1010 and 1731 cm^{-1}) suggests that there was a reaction between the amine groups and maleic anhydride forming the imide group, as shown in the mechanism in Figure 2. Essabir et al.²² also found a similar result in a study of the PA6/ABS blend compatible with SEBS-g-MA. It was observed in the FTIR spectrum of the PA6/SEBS-g-MA blend at a weight ratio of 84/16 that the stretching vibration of C-O-C (1120 cm^{-1}) strongly decreases when SEBS-g-MA is added to PA6. The decrease in this band was attributed to the reaction between PA6 and SEBS-g-MA.

3.4. Mechanical properties

According to the results shown in Figure 6 and Table 3, the 70Bio-HDPE/30PA6.10 blend exhibited an increase in the modulus of elasticity compared to the Bio-HDPE reference. This occurred because of the reinforcement effect of the polyamide, which has a higher modulus (2.09 GPa) and a higher yield stress (50.66 MPa). However, the reinforcing effect of the dispersed phase is highly inefficient, due to poor interfacial adhesion between these immiscible polymers. The low elongation at break of this blend confirms the incompatibility between the two phases, as observed in the SEM micrographs.

The results of the mechanical properties, in Figure 7 and Figure 8, showed that the addition of SEBS-g-MA and PE-g-MA promoted adhesion of the Bio-HDPE and PA6.10 phases. The increase in the content of these polymers functionalized with maleic anhydride led to an increase in elongation at break and this can be explained by the increase in the amount of anhydride groups available to react with PA6.10, promoting greater interfacial interaction.

It can be seen from the results that the presence of SEBS-*g*-MA improves impact strength and reduces the modulus of elasticity in relation to the values of the blends containing PE-*g*-MA. Blends with PE-*g*-MA did not show improvement in impact resistance, but there was an increase

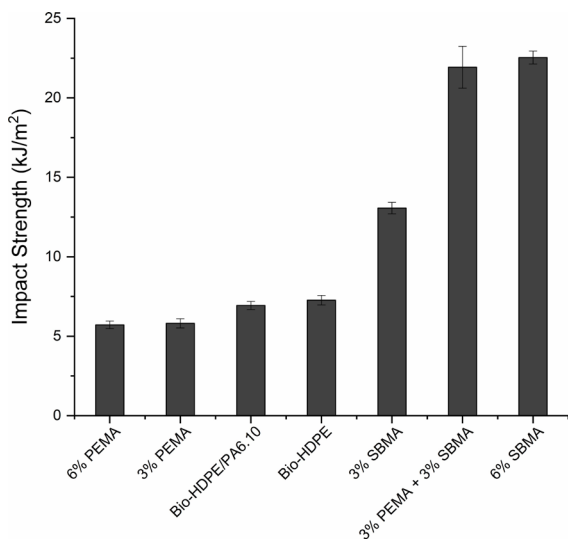


Figure 8. Impact strength of the blends.

in elongation at break compared to the Bio-HDPE/PA6.10 blend and an increase in yield stress and modulus of elasticity compared to Bio-HDPE.

Increasing the SEBS-*g*-MA content from 3% to 6% improves elongation at break and impact strength but decreases yield strength and modulus of elasticity. SEBS is a triblock of Styrene-Ethylene/Butylene-Styrene. The Ethylene/Butylene block is the soft phase. As shown by the works by Wilkinson et al.^{23,24}, and Kim et al.²⁵, from TEM images, there is a tendency for SEBS-*g*-MA to be localized around PA phase droplets, illustrated in Figure 9.

Probably the PE-*g*-MA generates an interface with the same rigidity as the matrix. SEBS-*g*-MA forms a soft interface around PA6.10, which implies lower resistance to tensile deformation. This results in a reduction in the modulus of elasticity of the blend. The increase in impact resistance observed in the blends with 3% PE-*g*-MA + 3% SEBS-*g*-MA and with 6% SEBS-*g*-MA may be related to the plastic deformation of the Bio-HDPE matrix together with the energy dissipation promoted by the detachment of rubber particles.

The blend containing 3% PE-*g*-MA + 3% SEBS-*g*-MA showed interesting results. The modulus of elasticity and yield stress were maintained close to the values obtained for pure Bio-HDPE, but with a gain of about 67% in impact resistance, an increase like that observed in the blend with 6% of SEBS-*g*-MA.

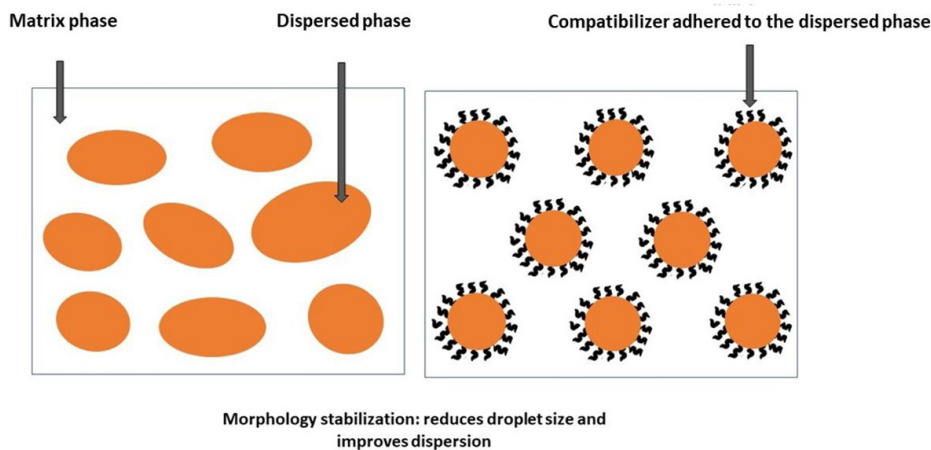


Figure 9. A schematic representation of the compatibilizing agent's action in immiscible blends.

Table 3. Values of tensile modulus, yield strength, elongation at break, and Impact strength of the blends.

Sample	Tensile modulus (GPa)	Yield strength (MPa)	Elongation at break (%)	Impact strength (kJ/m ²)
PA6.10	2.09±0.06	50.66±1.21	97.91±53.96	*
Bio-HDPE/PA6.10	1.71±0.01	23.82±0.33	11.46±1.27	6.93±0.26
3% PEMA	1.65±0.02	26.94±0.30	36.33±7.67	5.81±0.29
6% PEMA	1.65±0.01	27.20±0.23	50.48±6.86	5.72±0.24
3% SBMA	1.47±0.02	24.28±0.36	39.01±7.89	13.07±0.36
3% PEMA + 3% SBMA	1.46±0.01	24.19±0.10	56.32±12.56	21.93±1.32
6% SBMA	1.33±0.02	22.57±0.26	85.37±12.64	22.54±0.41
Bio-HDPE	1.47±0.02	23.41±0.36	206.99±10.14	7.27±0.30

* Impact strength PA6.10 = 6.5 kJ/m² (30)

4. Conclusions

This work studied the effect of adding PE-g-MA and SEBS-g-MA on the morphology, mechanical properties, and thermal properties of the blend of biopolyethylene with biopolyamide 6.10 (Bio-HDPE/PA6.10). The resulting morphology indicated an increase in the interaction between the matrix and the dispersed phase in the presence of these functionalized polymers. Furthermore, PE-g-MA and SEBS-g-MA acted stabilizing morphology reducing the size of the PA6.10 dispersed phase. The results obtained by FTIR suggest the occurrence of a chemical reaction between the maleic anhydride groups and the terminal amino groups of the polyamide, due to the decrease of absorption bands characteristic of the anhydride group in the spectra referring to the blends. The chemical reaction leads to the formation of the copolymer *in situ* during melt blending.

The presence of SEBS-g-MA improves toughness and reduces the modulus of elasticity in relation to the values of blends containing PE-g-MA. The blend with PE-g-MA showed higher modulus of elasticity than that pure Bio-HDPE. A synergistic effect of PE-g-MA and SEBS-g-MA was observed when 3% of both, PE-g-MA, and SEBS-g-MA, were added to the blend, showing a balance of mechanical properties. Thermal analysis showed changes in the crystallization behavior of both the dispersed phase and the matrix, suggesting greater interaction between the blend components and the occurrence of chemical reactions between maleic anhydride groups and amine groups.

5. Acknowledgments

We would like to thank Evonik Industries for donating Biopolyamide 6.10, Kraton for donating SEBS-g-MA, and Arkema for donating PE-g-MA. We are also grateful to CNPQ for opening public notice n° 18/2013 MCTI/CNPq/SPM-PR/Petrobras through which Bio-HDPE was acquired. We would like to express our gratitude to the Department of Materials Engineering at the Federal University of Sergipe and to Senai-Cimatec for providing the necessary infrastructure to advance this research initiative, and to Foundation for the Support of Research and Technological Innovation of the State of Sergipe (FAPITEC) for granting a research grant through public notice n° 04/2021.

5. References

- Pantani R, Turng LS. Manufacturing of advanced biodegradable polymeric components. *J Appl Polym Sci.* 2015;132(48):42889.
- Tarazona NA, Machatschek R, Balucho J, Castro-Mayorga JL, Saldarriaga JF, Lendlein A. Opportunities and challenges for integrating the development of sustainable polymer materials within an international circular (bio)economy concept. *MRS Energy and Sustainability.* 2022;9(1):28-34.
- Letcher TM. *Plastic waste and recycling.* 1st ed. Cambridge: Elsevier Inc; 2020.
- Phillips JH. *Biorenewable polymers.* In: Grubbs RH, Wenzel AG, O'Leary DJ, Khosravi E, editors. *Handbook of metathesis.* 2nd ed. Germany: Wiley-VCH; 2015. p. 357-374.
- McKeen LW. *Film properties of plastics and elastomers.* 1st ed. Cambridge: Elsevier Inc; 2017.
- Huang H. *Microbial ethanol, its polymer polyethylene, and applications.* In: Chen G, editor. *Plastics from bacteria: natural functions and applications.* 1st ed. Heidelberg: Springer Berlin; 2010. p. 389-404.
- Tarani E, Papageorgiou DG, Valles C, Wurm A, Terzopoulou Z, Bikiaris DN, et al. Insights into crystallization and melting of high density polyethylene/graphene nanocomposites studied by fast scanning calorimetry. *Polym Test.* 2018;67:349-58.
- Pagacz J, Raftopoulos KN, Leszczyńska A, Pielichowski K. Bio-polyamides based on renewable raw materials: glass transition and crystallinity studies. *J Therm Anal Calorim.* 2016;123(2):1225-37.
- Campbell IR, Lin MY, Iyer H, Parker M, Fredricks JL, Liao K, et al. Progress in sustainable polymers from biological matter. *Annu Rev Mater Res.* 2023;53:81-104.
- Nwabunma D, Kyu E. *Polyolefin blends.* 1st ed. New Jersey: John Wiley & Sons; 2007.
- Quiles-Carrillo L, Montanes N, Fombuena V, Balart R, Torres-Giner S. Enhancement of the processing window and performance of polyamide 1010/bio-based high-density polyethylene blends by melt mixing with natural additives. *Polym Int.* 2020;69(1):61-71.
- Ararat CA, Percino MJ, Murillo EA. Compatibilization of LDPE/PA6 by using a LDPE functionalized with a maleinized hyperbranched polyester polyol. *Macromol Res.* 2020;28(3):203-10.
- Ou Y, Lei Y, Fang X, Yang G. Maleic anhydride grafted thermoplastic elastomer as an interfacial modifier for polypropylene/polyamide 6 blends. *J Appl Polym Sci.* 2004;91(3):1806-15.
- Filippi S, Yordanov H, Minkova L, Polacco G, Talarico M. Reactive compatibilizer precursors for LDPE/PA6 blends, 4: maleic anhydride and glycidyl methacrylate grafted SEBS. *Macromol Mater Eng.* 2004;289(6):512-23.
- Filippi S, Minkova L, Dintcheva N, Narducci P, Magagnini P. Comparative study of different maleic anhydride grafted compatibilizer precursors towards LDPE/PA6 blends: morphology and mechanical properties. *Polymer (Guildf).* 2005;46(19):8054-61.
- Filippi S, Chiono V, Polacco G, Paci M, Minkova LI, Magagnini P. Reactive compatibilizer precursors for LDPE/PA6 blends, 1: Ethylene/acrylic acid copolymers. *Macromol Chem Phys.* 2002;203(10-11):1512-25.
- El-Wakil AA, Moustafa H, Abdel-Hakim A. Effect of LDPE-g-MA as a compatibilizer for LDPE/PA6 blend on the phase morphology and mechanical properties. *Polym Bull.* 2022;79(1):2249-62.
- Wu Y, Zhang H, Shentu B, Weng Z. In situ formation of the core-shell particles and their function in toughening PA6/SEBS-g-MA/PP blends. *Ind Eng Chem Res.* 2017;56(41):11657-63.
- Isayev AI. *Encyclopedia of polymer blends: structure.* Germany: Wiley-VCG; 2016.
- Piorowska E, Rutledge GC. *Handbook of polymer crystallization.* New Jersey: John Wiley & Sons, Inc; 2013.
- Liu H, Wu Q, Zhang Q. Preparation and properties of banana fiber-reinforced composites based on high density polyethylene (HDPE)/Nylon-6 blends. *Bioresour Technol.* 2009;100(23):6088-97.
- Essahir H, El Mechtali F, Nekhlouai S, Raji M, Bensalah M, Rodrigue D, et al. Compatibilization of PA6/ABS blend by SEBS-g-MA: morphological, mechanical, thermal, and rheological properties. *Int J Adv Manuf Technol.* 2020;110:1095-111.
- Wilkinson AN, Clemens ML, Harding VM. The effects of SEBS-g-maleic anhydride reaction on the morphology and properties of polypropylene/PA6/SEBS ternary blends. *Polymer (Guildf).* 2004;45(15):5239-49.
- Wilkinson AN, Laugel L, Clemens ML, Harding VM, Marin M. Phase structure in polypropylene/PA6/SEBS blends. *Polymer (Guildf).* 1999;40(17):4971-5.
- Kim GM, Michler GH, Gahleitner M, Mülhaupt R. Influence of morphology on the toughening mechanisms of polypropylene modified with core-shell particles derived from thermoplastic elastomers. *Polym Adv Technol.* 1998;9(10-11):709-15.